Sensors & Actuators: B. Chemical 332 (2021) 129484

Contents lists available at ScienceDirect

Sensors and Actuators: B. Chemical

journal homepage: www.elsevier.com/locate/snb

Selective *Campylobacter* detection and quantification in poultry: A sensor tool for detecting the cause of a common zoonosis at its source

Stella Givanoudi [a,b], Peter Cornelis [a], Geertrui Rasschaert [b], Gideon Wackers [a], Heiko Iken [c], David Rolka [c], Derick Yongabi [a], Johan Robbens [b], Michael J. Schöning [c], Marc Heyndrickx [b,d], Patrick Wagner [a,*]

[a] KU Leuven, Department of Physics and Astronomy, Laboratory for Soft Matter and Biophysics, Celestijnenlaan 200 D, B-3001, Leuven, Belgium
[b] Flanders Research Institute for Agriculture, Fisheries and Food, ILVO, Animal Sciences Unit & Technology and Food Unit, Burgemeester Van Gansberghelaan 92, B-9820, Merelbeke, Belgium
[c] Aachen University of Applied Sciences, Institute of Nano- and Biotechnologies INB, Heinrich-Mußmann-Straße 1, D-52428, Jülich, Germany
[d] Ghent University, Department of Pathology, Bacteriology and Avian Diseases, Salisburylaan 133, B-9820, Merelbeke, Belgium

ARTICLE INFO

Keywords:
Campylobacter species
Poultry farming
Zoonosis
Biomimetic sensors
Surface-imprinted polymers
Heat-transfer method

ABSTRACT

Thermotolerant *Campylobacter* bacteria, most notably *Campylobacter jejuni* and *Campylobacter coli*, are a major cause of human foodborne gastroenteritis, which is usually related to consumption of contaminated poultry. In this work, we present a sensor and the associated assay for the on-site detection of the prevalent species *C. jejuni* and *C. coli*. The sensor uses surface-imprinted polymer (SIP) layers as selective, biomimetic recognition elements in combination with a modified heat-transfer method (M-HTM) as a label-free, quantitative readout principle. The selectivity for *C. coli* and *C. jejuni* was evaluated against six other morphologically similar *Campylobacterales* species, confirming that the sensor is selective at species level while responding uniformly to different strains within the same species. For the relevant matrix, that is chicken cecal droppings suspended in PBS buffer, the detection limits are 1.1×10^3 CFU/mL for *C. coli* and 2.7×10^4 CFU/mL for *C. jejuni*, which is both low enough for a meaningful diagnostic test. The sensor concept requires only a minimum of sample preparation and a given concentration can be measured within less than one hour: Both are important assets for on-site detection such as on a poultry farm or in a slaughterhouse, keeping in mind that *Campylobacter* detection with established methods in analytical laboratories takes 2–4 days for obtaining the result.

1. Introduction

Thermotolerant *Campylobacter* (hereafter called *Campylobacter*), the causative agent of campylobacteriosis, is a major health concern globally. The World Health Organization (WHO) estimates that in 2010 *Campylobacter* was responsible for 166 million illness cases, including 96 million food-related illnesses, and it was the second most prevalent foodborne pathogen, after the norovirus [1]. Within the European Union, *Campylobacter* is responsible for the majority of bacterial foodborne gastroenteritis cases with a notification rate of 64.8 per 10,000 population and year [2]. Humans are exposed to *Campylobacter* through consumption of contaminated food, person-to-person transmission and direct contact with contaminated animals (domesticated and wild).

Campylobacter has been isolated from poultry [3], cattle [4], pigs [5], sheep [6], cats and dogs [7]. During slaughtering of chicken, the intestine is frequently ruptured, which leads to leakage of intestinal (and cecal) contents onto the carcass and the meat [8]. Undercooked poultry (broiler chicken, turkeys, ducks and geese) and milk are the primary sources of *Campylobacter* contamination [2], although it is possible to eliminate *Campylobacter* by heating to temperatures above 70 °C [9]. The European Food Safety Authority (EFSA) estimates that chicken is responsible for 50–80 % of campylobacteriosis cases, making them a major reservoir for infection [10]. Additionally, poultry-meat consumption is expected to increase further from 124.6 megatons (worldwide) in 2019 to 140.2 megatons in 2028 [11]. The production needs to rise accordingly with the strongest increase expected for the developing countries [12]. This creates a fertile ground for *Campylobacter* infections and highlights the need for monitoring foodborne pathogens in animal- and food-producing facilities. To prevent *Campylobacter* contamination during food production, the meat industry will need novel technologies

* Corresponding author at: KU Leuven, Laboratory for Soft Matter and Biophysics, Celestijnenlaan 200 D, B-3001, Leuven, Belgium.
E-mail address: patrickhermann.wagner@kuleuven.be (P. Wagner).

https://doi.org/10.1016/j.snb.2021.129484
Received 23 November 2020; Received in revised form 5 January 2021; Accepted 6 January 2021
Available online 11 January 2021

to monitor and restrict the pathogen.

Conventional methods for the detection of *Campylobacter*, such as polymerase chain reaction PCR tests [13], qPCR [14], and cultivation [15] are established and sensitive. For example, PCR has a limit of detection (LoD) of 50 CFU/mL while qPCR reaches a LoD of 3.3 log CFU per carcass; CFU denotes colony-forming units. Nonetheless, these methods require trained staff, analytical-laboratory facilities, and costly reagents. This also holds for cell-culture methods based on the ISO standard (ISO 10272-1:2017), which take 2–4 days from sample preparation to result. Hence, it is difficult to analyze large sample batches without delay by using the established techniques. To fulfill high food-safety demands, we need detection tools that are fast, low-cost, and applicable directly at the relevant location such as farms, slaughterhouses or food factories.

Biosensor technology is working towards on-site testing: Table 1 provides an overview on research-type biosensors that were developed for *Campylobacter* detection [16]. Most of these assays use antibodies as receptors that are coupled to optical, electro-optical, and electro-chemical transducers; some of these techniques require additional labelling chemistry. A limited number of on-site tests for *Campylobacter* detection is already available commercially [17–21]. However, these are single-use tests that suffer either from a long response time (up to 49 h) or require a high bacterial load (*i.e.* detection is only possible in highly *Campylobacter*-colonized broiler flocks).

In the present work, we have developed surface-imprinted polymer (SIP) receptors for *Campylobacter*. SIPs are biomimetic receptors that have been used successfully to detect bacteria [22–25], yeast [26], mammal cells [27,28], viruses [29,30], and proteins [31]. SIPs, a subtype of molecularly imprinted polymers, are imprinted only at the surface to allow for facile template extraction after imprinting [32,33]. SIP receptors can be combined with various transducers, including surface plasmon resonance [25,34], microbalances [25,35], impedance spectroscopy [36], and thermal detection [27,37]. Compared to antibodies, SIPs have a low fabrication cost and can be regenerated multiple times without losing affinity. It is feasible to deposit SIPs on various chip materials, including glass, silicon, and metals, which enables a broad application range. Although they do not yet reach the selectivity of antibodies, there is rapid progress in enhancing selectivity as seen for instance in blood-group typing [28], distinguishing cancer-cell lines [27], and recent work on *Enterobacteriaceae* [23]. SIPs obtain their selectivity by two elements, being the geometrical matching between target cells and the imprints and complementarity of biochemical recognition functionalities: During imprinting, phospholipid fragments of the template cells are transferred to the polymer where they serve as anchoring points when binding target cells from solution. The relevance of phospholipid remnants was identified by scanning-electron microscopy, infrared spectroscopy (FTIR), and x-ray photoemission spectroscopy XPS [26]. The recognition mechanism of SIP layers has therefore also potential in cell-sorting [38,39]. In the present work on *Campylobacter*, we will take the selectivity of SIPs to test at several levels, including the strain, species, and order level to document the analytical capacity of this class of receptors in broad perspective. This entails also their *inclusivity*, describing to which extend receptors synthesized with a given template strain can also recognize bacteria of other strains within a species.

To quantify the binding of target cells, we combine SIP coatings on stainless-steel chips with the thermal detection principle of the heat-transfer method HTM, which is explained in its basic version in refs. [48–50]. In brief, HTM measures the thermal resistance R_{th} of a solid-liquid interface, which depends sensitively on the presence (or absence) of target particles such as cells at this interface. The main elements are a heat source at the backside of the sensor chip, whose temperature T_1 is kept constant (*e.g.* 37.0 °C) using a PID (proportional, integral, derivative) controller, and a thermocouple that measures the temperature T_2 of the supernatant liquid. A schematic cross section of a HTM device is provided in Fig. 1. Together with the heating power P, we obtain the thermal resistance R_{th} according to Eq. (1):

$$R_{th} = \frac{T_1 - T_2}{P} \left[\frac{°C}{W}\right] \quad (1)$$

Binding of cells to the interface between the SIP coating and the liquid enhances R_{th} in a concentration-dependent way because phospholipid bilayers have high thermal resistance [51]. Without further optimization, HTM can reach a lower LoD in the order of 10^4 CFU/mL for *Escherichia coli*- and *Staphylococcus aureus* when combined with SIP-type receptors [24]. Other applications of HTM include the detection of single-nucleotide polymorphisms in DNA [52], monitoring the proliferation and quality of cell cultures [53,54], and detecting phase transitions in lipid vesicles [55]. The HTM device used in the present work is a technical upgrade (denoted as *modified heat-transfer method*, M-HTM) in which a calibrated, planar gold meander provides the heating power P and measures the backside temperature T_1 of the chip. This meander combines the hitherto individual elements, a power

Table 1
Biosensors for the detection of *Campylobacter*. CFU: Colony forming units, SPR: surface plasmon resonance, FRET: Förster resonance energy transfer, TIRF: total internal reflection fluorescence, M-HTM: modified heat-transfer method.

Target	Bioreceptor /Detection Method	LoD (CFU/mL)	Application / Medium	Labelling	Reference
C. jejuni	Antibody / SPR	10^3	PBS Broiler meat rinse	No	[40]
C. jejuni	Antibody / SPR	4×10^4	PBS	No	[41]
C. jejuni	Antibody / SPR	1.1×10^5	Apple juice	No	[42]
C. jejuni	Antibody / FRET	10 100	PBS Poultry liver samples	Yes	[43]
C. jejuni *C. coli*	Antibody / TIRF	9.7×10^2 7.8×10^5	PBS	Yes	[44]
C. jejuni		3.1×10^3 1.6×10^3 3.1×10^3	River water Ground turkey Carcass wash		
C. coli		1.6×10^6 7.8×10^5 7.8×10^5	River water Ground turkey Carcass wash		
Campylobacter spp	Antibody / Square-wave anodic stripping voltammetry	4×10^2	Tris–HCl buffer	Yes	[45]
C. jejuni	Antibody / Impedance spectroscopy	10^3	PBS	No	[46]
C. jejuni *C. coli*	Aptamer / Spectrophotometer	– –	Carcass wash	No	[47]
C. jejuni *C. coli*	SIP / M-HTM	6.6×10^3 1.0×10^3	PBS	No	This work, Fig. 3
C. jejuni *C. coli*		2.7×10^4 1.1×10^3	Chicken cecal droppings	No	This work, Fig. 4

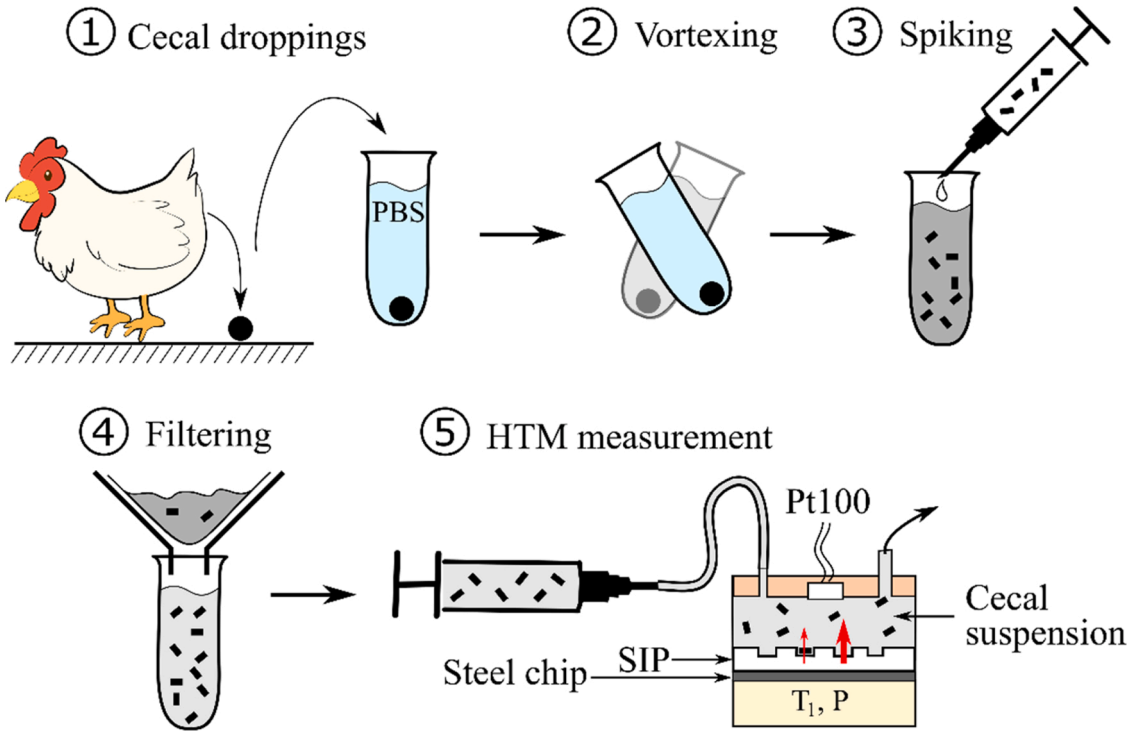

Fig. 1. Schematic workflow of establishing the dose-response curve of the sensor system, starting in step **1)** with dissolving *Campylobacter*-free cecal droppings in PBS buffer. Step **2)** is vortexing to homogenize the sample and step **3)** spiking with appropriate *Campylobacter* concentrations. After filtering in step **4)**, the cecal solution is introduced into the flow cell of the sensor in step **5)**, where bacteria that bind to the receptor layer (SIP) diminish the heat flow from the chip to the Pt100 temperature sensor embedded in the lid of the sample chamber. The heat flow is symbolized by red arrows. Note that components are not drawn to scale, short black bars symbolize the *Campylobacter* bacteria. (For interpretation of the references to colour in this figure legend, the reader is referred to the web version of this article).

resistor and a thermocouple to measure T_1, in a single element as described recently [23]. As a result, the device is compact (matchbox size), the heat flow is focused through the chip-to-liquid interface and, most importantly, there is a significant improvement in the signal-to-noise level of R_{th} data. M-HTM can therefore achieve a LoD as low as 100 CFU/mL (for *E. coli*) and enables to measure even weak binding signals, which is beneficial for cross-selectivity studies.

While there are several *Campylobacter* species, isolates from campylobacteriosis patients have revealed that *C. jejuni* and *C. coli* are predominant; *C. jejuni* counts for 84.4 % of the identified species and *C. coli* for 9.2 % as reported for the European Union [2]. Infections with other *Campylobacter* species are far less common and therefore, we chose to focus on detecting *C. jejuni* and *C. coli*. To quantify the cross-selectivity, the sensor response is measured for six different, potential competitor species that are morphologically similar to *C. jejuni* and *C. coli*. In addition, we evaluate the applicability of the sensor on cecal-droppings samples from chicken. In case of colonization, *Campylobacter* is abundant in the caecum of chicken with $10^6 - 10^8$ cfu/g and cecal droppings are easy to collect without slaughtering the animal [3,56]. Therefore, cecal droppings are the best choice of sample type to achieve maximum sensitivity when monitoring the bacterium in poultry farms.

2. Experimental section

2.1. Reagents and culture media

The culture media *Campylobacter* blood-free selective agar base CM0739B with CCDA selective supplement SR0155 (mCCDA), Mueller-Hinton Agar CM0337 and the micro-aerophilic atmosphere-producing CampyGen™ 3.5 L Sachets CN0035A were purchased from Thermo Fisher Scientific (Merelbeke, Belgium). The Sylgard 184 silicone-elastomer kit for preparing polydimethylsiloxane (PDMS) stamps was purchased from Malvom N.V. (Schelle, Belgium). All other reagents, *i.e.* acetone, isopropanol, ethanol, sodium dodecyl-sulfate (SDS), anhydrous tetrahydrofuran (THF), bisphenol A, phloroglucinol and 4,4′-diisocyanatodiphenyl-methane, NaCl, Na_2HPO_4, and KH_2PO_4 were purchased from Sigma-Aldrich (Diegem, Bel-gium). All chemicals had a purity of at least 99 %. The buffer, 10 × PBS (1.29 M NaCl, 0.061 M Na_2HPO_4, 14 mM KH_2PO_4, pH 7.4) was homemade and diluted to 1 × PBS (denoted as "PBS") with MilliQ water. Stainless-steel sheets (AISI 304, Finetubes, UK) cut into squares (10 × 10 × 0.2 mm^3) served as sensor chips.

2.2. Cell culturing and bacteria counting

The bacteria are four *C. coli* strains (MB3272, MB3363, MB4182, and C154a), three *C. jejuni* strains (MB3391, KC40, and C157a), *Campylobacter lari* (MB1268), *Campylobacter upsaliensis* (MB3264), *Helicobacter pullorum* (KC112), *Arcobacter butzleri* (P340), *Arcobacter cryaerophilus* (MB3234) and *Arcobacter skirrowii* (MB3238). *C. coli* C154a was isolated from pigs and *C. jejuni* C157a from broilers in 2018. More information on all species is summarized in the Supporting Material. The bacteria are kept in the MB collection of ILVO in horse-blood stocks at – 80 °C. *Campylobacter* and *Helicobacter* grew on mCCDA agar plates at 41.5 °C under microaerophilic conditions (5% O_2, 10 % CO_2, and 85 % N_2) overnight. *Arcobacter* was cultured on Mueller-Hinton agar plates, supplemented with 5 vol.% horse blood at 30 °C in microaerophilic conditions overnight. The bacteria were harvested from the agar plates by adding 2 mL PBS and softly rubbing the agar surface with a T-shaped cell spreader. This was repeated twice, then the bacterial suspension was filtered through sterile tissue paper to remove agar particles. The bacterial suspensions were washed with PBS to remove culture-medium residues, centrifuged at 7500 rpm for 10 min and re-suspended in PBS. The washing was repeated two additional times. All bacteria-related processes were performed in BSL-2 laboratories.

The concentration of all bacteria was calculated using the plate-count method: The initial bacterial suspension was diluted four times

in PBS with a dilution factor of 10 each (total dilution ratio: 1 to 10^4). We evenly spread 100 µl of the fourth dilution on mCCDA (for *Campylobacter* and *Helicobacter*) or Mueller-Hinton supplemented with 5 vol.% horse blood (for *Arcobacter*) agar plates and incubated them overnight at 41.5 °C in microaerophilic conditions. Finally, we counted the number of colonies per plate and calculated the initial concentrations based on the average colony number of three plates and the dilution factor.

2.3. Surface imprinting of polymer layers

We synthesized SIPs by imprinting *C. coli* (strain C154a) and *C. jejuni* (C157a) on polyurethane (PU) layers: PU was formed by dissolving 122 mg of 4,4′- diisocyanatodiphenyl-methane, 222 mg of bisphenol A and 25 mg of phloroglucinol in 500 µl anhydrous THF [27]. The mixture was stirred at 65 °C for 200 min under nitrogen atmosphere until the gelling point, and then diluted in a 1–5 ratio with THF. Then, the solution was applied on stainless-steel chips and spin-coated for 60 s at 2000 rpm (spin coater WS-650Mz-23NPPB, Laurell Technologies, North Wales, USA). In parallel, PDMS stamps (10 × 10 mm^2, 3 mm thickness) were covered with 700 µl bacterial suspension (10^6 CFM/mL) in PBS and the bacteria were allowed to sediment for 60 min. Thereafter, the cell-covered stamps were rotated for 30 s (2000 rpm) on the spin coater to remove excess liquid, resulting in a cell monolayer on the stamp surface. The stamps were then placed onto the still viscous PU layer (thickness *ca.* 1 µm) on the steel chips and the polyurethane was cured for 18 h at 65 °C under N_2 atmosphere. Finally, the stamps were removed from the chips, residues of the template bacteria were rinsed off with 1% SDS detergent and MilliQ water (each for 5 min), and the chips were blown dry with nitrogen gas. The chips were stored dry at room temperature until further use.

2.4. M-HTM sensor setup and data acquisition

The technical description of the M-HTM device, including the hardware and software, is given in ref. [23]. In brief, the setup consists of the actual sample compartment, a syringe pump (NE-500, ProSense, Oosterhout, The Netherlands), a Keithley 6221 current source and 2182A nanovoltmeter, a HP 34401A digital multimeter, and a laptop equipped with in-house developed LabView software. The sample compartment features a planar, meander-type heater (gold on glass) that also measures the backside temperature T_1 of the sensor chip, which is placed on top of the heater. Heat loss along the backside of the heater is minimized by thermal insulation. A rubber seal on top of the SIP chip defines the flow cell with 25 µl inner volume (5 × 5 × 1 mm^3). The top lid of the flow cell is made of titanium with integrated inlet- and outlet for the sample and a calibrated Pt100 sensor to measure the temperature T_2 of the liquid at 1.0 mm distance from the SIP layer. The meander heater itself is also calibrated and the accuracy of temperature readings is better than 0.1 °C. Together with the power P provided by the heater, one obtains R_{th} as defined in Eq. 1. During all experiments we kept T_1 at 37.0 ± 0.1 °C by PID control while the ambient temperature was 18.5 ± 0.5 ℃. The concentration-dependent R_{th} data were fitted with the dose-response function, see Eq. 2, which is implemented in the Origin™ software package [57].

$$R_{th} = A_1 + \frac{A_2 - A_1}{1 + 10^{(\log(C_0 - C)\cdot p)}} \quad (2)$$

C is the concentration of bacteria in CFU/mL while A_1 and A_2 stand for the bottom- and top asymptotes of the curve, respectively. C_0 is the concentration that corresponds to half of the total R_{th} response and p is the Hill slope.

2.5. Dose-response measurements

The dose-response curves were measured in two different ways: First with *Campylobacter* suspended in PBS and, second, with *Campylobacter* suspended in buffer solution containing chicken cecal droppings. The measurement with pure PBS started by filling the sample chamber twice with PBS and stabilizing T_1 at 37.0 ℃. The device was stabilized for 60 min after the second PBS injection to verify the reproducibility and stability of the baseline signal. Then, we injected *Campylobacter*-spiked PBS in increasing order of concentration from 5 × 10^3 to 5 × 10^5 CFU/mL (5, 10, 25, 50, 100, 250, and 500 × 10^3 CFU/mL). Each time, the injected volume was 1.0 mL (flow rate 0.2 mL/min, 5 min in total), which exceeds the flow-cell volume by 40 times to guarantee that the initial fluid was replaced completely. The bacteria were allowed to sediment and bind to the imprints for 20 min, after which we flushed the flow cell with 1.0 mL pure PBS to remove unbound bacteria that possibly affect the thermal conductivity of the liquid itself. After flushing, we waited again for 20 min, allowing the flow cell to return to thermal steady-state conditions before moving to the next-higher concentration. Due to the small flow-cell volume, the receptor surface was not regenerated between the subsequent exposures.

For the dose-response measurements on cecal samples, we used chicken cecal droppings from broiler flocks, which were verified to be *Campylobacter*-free as checked by cell-plating tests on mCCDA agar [58]. The samples were stored at – 80 ℃ until use and the workflow is illustrated in Fig. 1. We added 1.0 g of cecal samples to 10 mL of PBS and, to suspend the cecal droppings, the solution was mixed by vortexing at 2500 rpm for 2 min. Thereafter, the appropriate spiking doses were added to result in the same *Campylobacter* concentrations as with pure buffer. These solutions were filtered with Whatman™ filter paper (pore size: 20–25 µm, VWR, Oud Heverlee, Belgium), which allows bacteria to pass while larger, undissolved particles of the droppings are retained. With cell plating as a reference, we could prove that the filtration step does not decrease the actual *Campylobacter* concentration that is present in a sample. The dose-response measurements were performed in the same way as with PBS without the cecal matter. After measuring, all sensor components were decontaminated with 70 % ethanol and rinsing with MilliQ.

2.6. Selectivity and inclusivity measurements

For selectivity and inclusivity testing, the SIP receptors were imprinted with either *C. coli* (strain C154a) or *C. jejuni* (strain C157a) as described above, followed by testing their response to six *Campylobacterales* species, being *C. lari* (MB1268), *C. upsaliensis* (MB3264), *Helicobacter pullorum* (KC112), *Arcobacter butzleri* (MB3232), *A. cryaerophilus* (MB3234), and *A. skirrowii* (MB3238). In addition, we tested the *C. coli* imprinted SIPs against *C. jejuni* strain C157a and three *C. coli* strains (MB3272, MB3363, MB4182); *vice versa*, the *C. jejuni* imprinted SIPs were tested against *C. coli* strain C154a and two *C. jejuni* strains (MB3391, KC40). Each measurement was done with a new chip following the standard exposure protocol, however, with a uniform concentration of bacteria of 1.0 × 10^5 CFU/mL in PBS.

2.7. Acquisition of scanning-electron microscope (SEM) images

Due to the pathogenicity of *Campylobacter*, we used scanning-electron microscopy that allows imaging the SIPs under vacuum conditions. The SEM instrument was a JEOL JSM 7800 (Freising, Germany), equipped with a field-emission electron source and a secondary-electron detector. Prior to imaging, the SIP chips were metallized with a sputtered, 10 nm layer of Pt/Pd alloy (sputter coater JEOL JFC 2300) to compensate for the electrically insulating behavior of polyurethane. For SEM imaging, we chose magnifications of 16.000× (overview images) and 50.000× to zoom in at individual imprints.

3. Results and discussion

3.1. SEM imaging of Campylobacter imprints

The SEM images of *Campylobacter*-imprinted polymers are shown in Fig. 2. *Campylo-bacter* is Gram negative with a spiral rod shape, its length varies between 0.5–5 μm and the width is 0.2 – 0.8 μm [59]. The dimensions of *C. jejuni* shown in Fig. 2A agree with literature, which also holds for the imprinted, empty cavities in Fig. 2B and C, becoming visible after template extraction. The areal density of cavities, as determined from overview scans, is *ca.* 1.5×10^4 cavities/cm^2 for *C. coli* and 1.3×10^4 cavities/cm^2 in case of *C. jejuni*. For comparison, using the same imprinting protocol for *E. coli* resulted in SIPs with more than 10^6 imprints per cm^2 [23]. We attribute the low imprint density in the present case to the fact that *Campylobacter* cells tend to aggregate in solution, which decreases the number of resulting, unique cavities on the SIP surface. Furthermore, the yield of *Campylobacter* colonies during plate culturing is lower than for *E. coli*, which is cultured in suspension.

Another effect at play is shown in Fig. 2D, where coccoids with 0.8 μm diameter are visible on the SIP surface. This indicates that *Campylobacter* template cells encounter stress during the imprinting, where temperature rises to 65 °C in the curing step. It is reported that *C. jejuni* can change into its coccoid form above 60 ℃ [60], while the transition from helical to coccoid morphology can also be induced by other stress factors such as oxidative and aerobic stress, osmotic shock, starvation, and entry into the stationary phase [61–63].

3.2. Dose-response of Campylobacter in PBS buffer

Fig. 3A shows the R_{th} response of the sensor with a *C. coli* imprinted SIP layer upon exposure to the same target strain. Here, we followed the protocol as described in the **Experimental Section**, starting with establishing the baseline and its standard deviation σ with pure PBS and then administering increasingly higher *Campylobacter* concentrations from 5 to 500 × 10^3 CFU/mL in PBS. As illustrated in Fig. 3B, each exposure to a given concentration consists of four steps: i) Injection of the sample, ii) sedimentation, iii) flushing with pure PBS to remove unbound cells, and iv) the thermal equilibration.

The spikes in the R_{th} signal indicate that fluid at room temperature is injected into the flow cell, causing a temporary overshooting of the signal. To obtain the dose-response curve, we utilized the R_{th} data collected in the last 5 min of the sedimentation- and equilibration phases (datasets B and C). Here, the internal temperature distribution of the stagnant liquid in the flow cell is again in equilibrium. Fig. 3C shows the stepwise increase of R_{th} with increasing *C. coli* concentration, illustrating that bound bacteria do indeed enhance the thermal interface resistance. The data points are averages of the data obtained as datasets B and C, respectively; the error bars are the standard deviations.

Furthermore, it is interesting to note that after PBS flushing, R_{th} is slightly but systematically higher than before flushing when unbound bacteria are still present in the liquid; this agrees with earlier observations on *E. coli* sensing [23]. Tentatively, it can be understood by the "nanoliquid effect" that micro- and nanoparticles, suspended in very small concentration in a liquid, lower its thermal resistivity [64,65].

Fig. 3D shows the dose-response curve of the sensor for *C. jejuni* with the receptor layer being imprinted with the same *C. jejuni* strain. The calibration curves for both species show similar features such as the sigmoidal curvature and both can be fitted with the dose-response model of Eq. 2. The baseline value is in both cases almost identical, which indicates the reproducibility of the concept. For the highest concentration

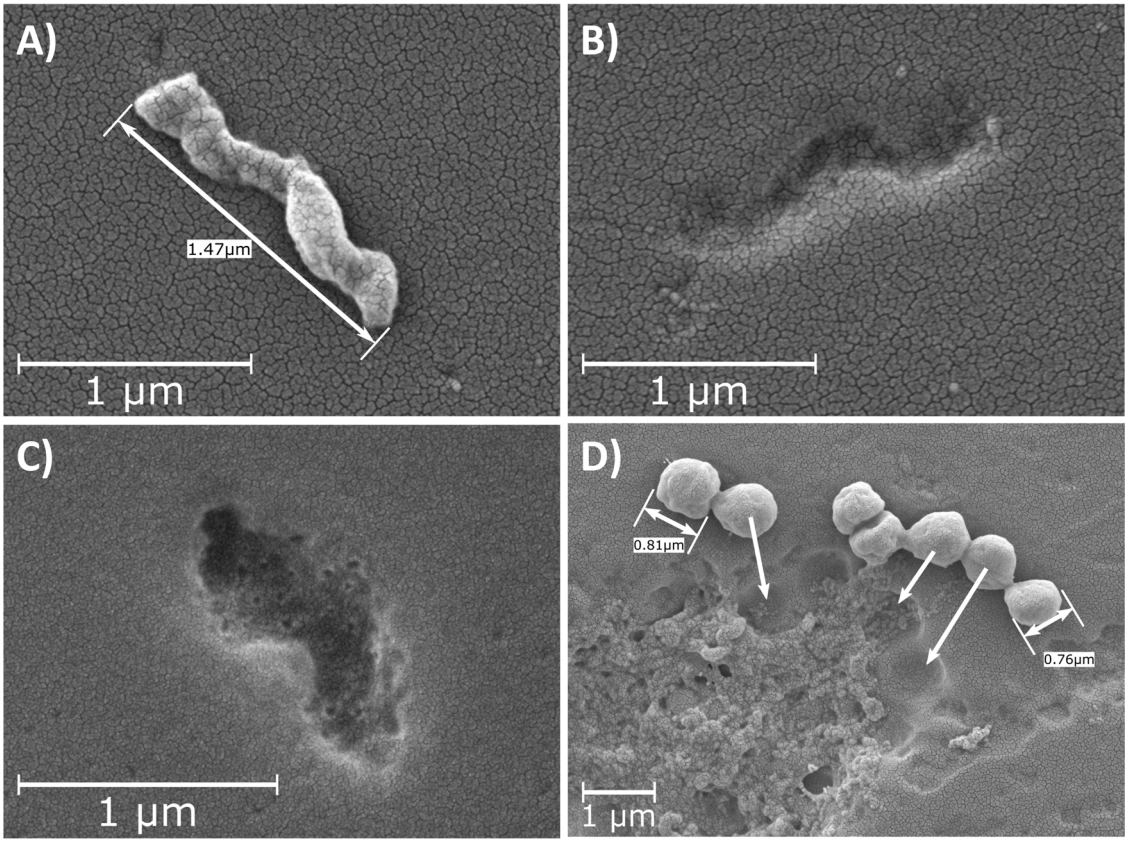

Fig. 2. SEM images of A) *Camylobacter jejuni* cell, still sticking to its corresponding imprint, on a PU-based SIP layer at 50,000× magnification. B) Individual, imprinted cavity after extraction of the *C. jejuni* template at 50,000× magnification. C) Individual cavity obtained by imprinting with *C. coli*, 50,000× magnification. D) Empty coccoid cavities and coccoid forms of *C. jejuni* on a SIP imprinted with *C. jejuni*, magnification 16,000×. In all images, imprinting was done on the surface of polyurethane on stainless-steel chips. *C. jejuni* and *C. coli* are strains C157a and C154a, respectively. The granular surface morphology is due to a metallization layer.

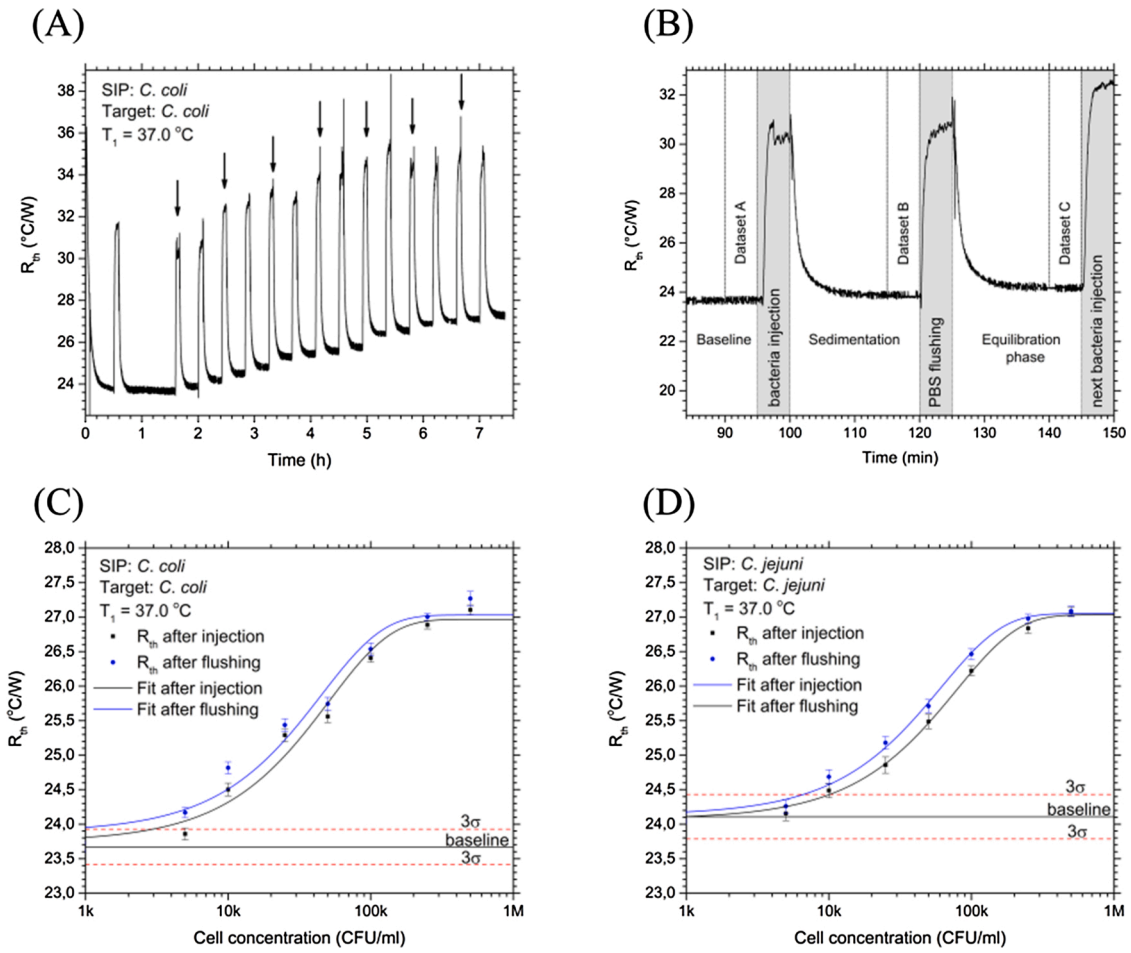

Fig. 3. A) Dose-response measurement performed with a SIP imprinted with *C. coli* according to the sequence described in the Experimental Section. Spikes marked with an arrow refer to injection of *C. coli* spiked PBS, starting with 5×10^3 CFU/mL. Unmarked spikes refer to flushing with pure PBS. B) Expanded view of the exposure to 5×10^3 CFU/mL, illustrating the moments of taking datasets and the influence of PBS flushing on the R_{th} signal. This scheme was maintained for all concentrations. C) and D) Dose-response curves for C. coli (panel C) and *C. jejuni* (panel D). The solid lines were fitted with the dose-response function Eq. 2 and have $R^2 > 0.98$ in all cases. Note that the R_{th} signal after flushing (blue lines) is higher than after exposure (black lines). The red dotted line corresponds to the 3σ level, with σ being the standard deviation of the baseline. (For interpretation of the references to colour in this figure legend, the reader is referred to the web version of this article).

(500×10^3 CFU/mL) and after flushing, the relative increase of the R_{th} signal is 15.2 % for *C. coli* and 12.3 % in case of *C. jejuni*, which seems related to the slightly higher areal density of *C. coli* imprints. The detection limit was calculated from the fit curves as the lowest concentration that generates a signal exceeding the 3σ level: For the PBS matrix and after flushing, the LoD is 1.0×10^3 CFU/mL for *C. coli* and 6.6×10^3 CFU/mL in case of *C. jejuni*. This is in the same order as for most antibody-based *Campylobacter* sensors, see Table 1. The lowest measured concentrations for which the signal clearly exceeded the 3σ threshold are 5×10^3 CFU/mL (*C. coli*) and 1.0×10^4 CFU/mL for *C. jejuni*. In case of the previously studied *E. coli*, we attribute the low LoD of 100 CFU/mL to the considerably higher density of available binding sites [23].

3.3. Dose-response of Campylobacter in chicken cecal droppings samples

Next, we evaluated the performance of the sensor in detecting *C. coli* and *C. jejuni* in spiked cecal-droppings samples dissolved in PBS. As outlined above, there was no other sample pretreatment than filtering and, since the cecum is the main multiplication site for *Campylobacter,* cecal droppings are used in veterinary medicine to detect colonization with these bacteria in chicken flocks [66]. The R_{th} response of a *C. coli* imprinted SIP is given in Fig. 4A, displaying the same stepwise increase of R_{th} as a function of concentration as in the dose-response calibration with PBS. In addition, we examined the effect of the cecal solution itself on the R_{th} signal by adding two extra steps in the dose-response measurement, see Fig. 4B: After the initial stabilization of the device with pure PBS (dataset A), the flow cell was filled with *Campylobacter*-free cecal solution (dataset D), which was replaced again by pure PBS (dataset E). All datasets were collected under equilibrium conditions for 5 min. Upon exchanging PBS by the cecal solution, R_{th} increases by less than 0.1 °C/W and a second increase in this order occurs after replacing the cecal solution again with pure PBS. Hence, there is no significant difference and, within the accuracy of the technique (± 0.3 °C/W), the thermal properties of cecal solution and PBS are equal. This is reasonable since the cecal solution consists for 90 % of PBS and the nanoliquid effect mentioned above is not known for high particle concentrations. This indicates that the *Campylobacter* SIPs do not bind the bacteria that are inherently present in the cecal microbiome and an overview on the microorganisms in poultry intestines can be found in ref. [67].

The dose-response curves of the sensor exposed to suspensions of *C. coli* and *C. jejuni* are plotted in Fig. 4C (*C. coli*) and D (*C. jejuni*). In contrast to the dose-response measurement in pure PBS (see Fig. 3C, D), the baseline is defined by dataset E, *i.e.* after the initial exposure to the *Campylobacter*-free cecal sample to take potential fouling effects into account. The fit function for the dose-response behavior is again

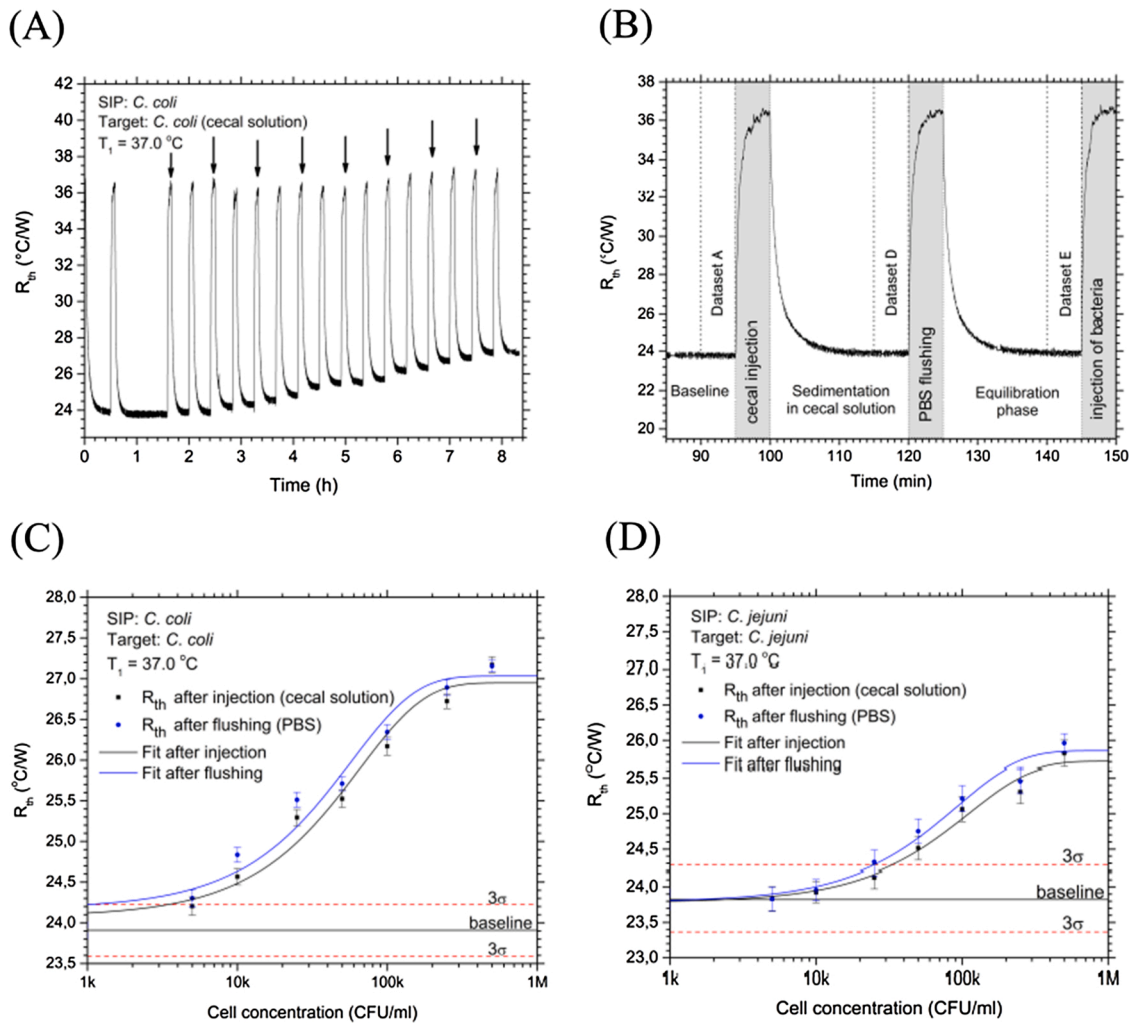

Fig. 4. A) Dose-response measurement performed with a *C. coli* imprinted SIP layer when binding the target bacteria from cecal solution. Spikes on the curve indicated with an arrow refer to the injection of cecal solution, starting with a *Campylobacter*-free cecal sample. Non-marked spikes refer to flushing with PBS. B) Enlarged view of the initial sequence PBS → cecal sample → PBS; the datasets A, D, E show that PBS and cecal solution have the same thermal resistance. C) Dose-response curve for *C. coli* and D) for *C. jejuni*. The fit curves calculated with Eq. 2 have R^2 values of at least 0.94 in all cases. The red dotted lines denote the 3σ interval around the baseline that was determined with the exposure step to Campylobacter-free cecal solution. (For interpretation of the references to colour in this figure legend, the reader is referred to the web version of this article).

calculated with Eq. 2. The calculated LoD values, after PBS flushing, are 1.1×10^3 CFU/mL for *C. coli* and 2.7×10^4 CFU/mL for *C. jejuni*, both bound to the receptor layer from cecal solution. As expected, these detection limits are higher than when binding the bacteria from pure PBS, see Fig. 3. The measured concentrations for which the signal clearly exceeds the 3σ level are 5.0×10^3 CFU/mL (*C. coli*) and 5.0×10^4 CFU/mL for *C. jejuni*.

3.4. Cross-selectivity and inclusivity of Campylobacter SIPs

The final part of this work studies the cross-selectivity of SIPs imprinted with *C. coli* (strain C154a) and SIPs imprinted with *C. jejuni* (strain C157a). Six other bacterial species were examined using the M-HTM sensor, being *C. lari*, *C. upsaliensis*, *A. butzleri*, *A. cryaerophilus*, *A. skirrowii,* and *H. pullorum*. In addition, three *C. coli* strains (MB3272, MB3363, and MB4182) and two *C. jejuni* strains (MB3391 and KC40) were used to test the inclusivity of the SIPs. Inclusivity denotes the ability of the receptors, imprinted with a specific strain, to respond equally to genetically different strains of the same species. The genus *Campylobacter* contains other human pathogens such as *C. lari* and *C. upsaliensis*, which have spiral-rod shape, 0.2 – 0.8 μm width and 0.5–5 μm length [59]. Similar to *Campylobacter*, the genera *Helicobacter* and *Arcobacter* also contain *Campylobacter*-like zoonotic pathogens: *H. pullorum*, a slightly curved bacilliform bacterium (0.3 – 0.5 μm wide, 3–4 μm long), has been isolated from the cecum of poultry [68], and it is associated with gastroenteritis in humans [69]. Also, *Arcobacter*, a member of the *Campylobacteraceae* family, is morphologically similar to *Campylobacter* (spirally curved shape, 0.2 – 0.9 μm wide, 1–3 μm long) and found in poultry as well [70].

For these tests, we used for all combinations of SIPs and target bacteria the same exposure scheme that is exemplarily illustrated in Fig. 5A for the case of a SIP imprinted with *C. jejuni* (strain C157a) as a template and *C. jejuni* (strain MB3391) as a target. In all experiments, we used freshly prepared receptor chips and PBS as a medium to avoid any potential influence of a complex matrix. After establishing the baseline, the target cells were injected at a uniform concentration of 1.0×10^5 CFU/mL and allowed to sediment and to bind to the SIP. Then, we flushed the flow cell with pure PBS and registered the persistent increase ΔR_{th} with respect to the baseline when the temperature distribution in the flow cell was again in steady state.

The strongest ΔR_{th} response was obtained for the symmetrical combinations: Using *C. jejuni* strain C157a as a template and target resulted in $\Delta R_{th} = 2.34$ °C/W; for the *C. coli* strain C154a as template and target we obtained 2.88 °C/W. For easier comparison, we normalized these

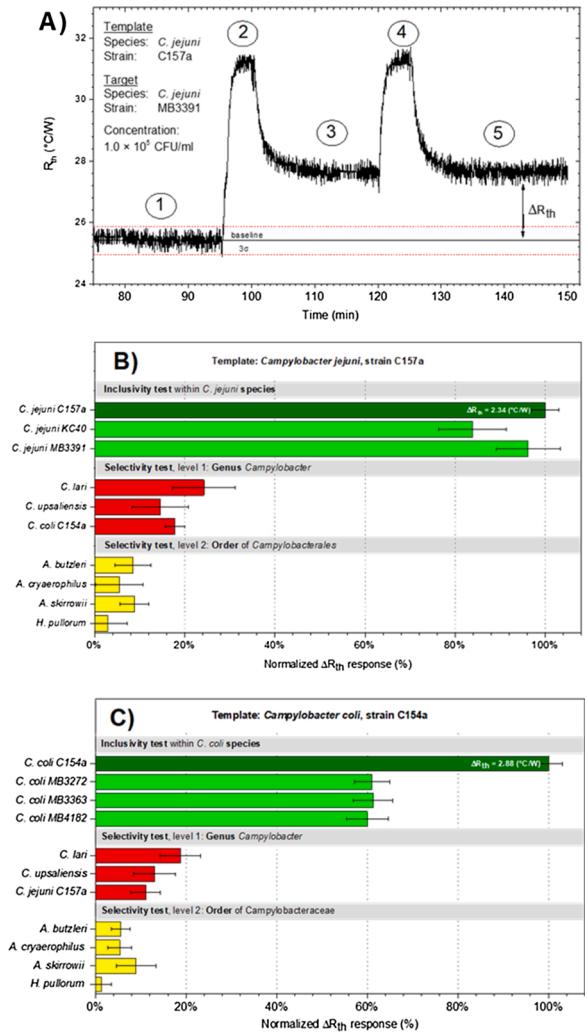

Fig. 5. A) Exemplary cross-response measurement of a SIP imprinted with *C. jejuni* C157a in the following steps: 1) Establishing the baseline and the 3σ interval in PBS, 2) injection of *C. jejuni* strain MB3391 at a concentration of 1.0 × 10^5 CFU/mL, 3) sedimentation and 4) flushing with pure PBS. The cross-response ΔR_{th}.is registered at the end of step 5) and normalized to the specific response, set as 100 %. This protocol was applied to all species and strains. The selectivity and inclusivity profiles are shown in panel B) for *C. jejuni* (C157a) and in C) for C. coli (154a): The data, given as green bars, show that SIP receptors are inclusive for strains within the same species. The sensor response to other species within the *Campylobacter* genus (red bars) is typically only 15 – 20 %. For other members of the order of Campylobacterales, shown as yellow bars for *Arcobacter* and *Helicobacter*, the signal stays below the 3σ level. Error bars represent the standard deviations from step 5) in panel A). (For interpretation of the references to colour in this figure legend, the reader is referred to the web version of this article).

specific responses to 100 %, which is illustrated in Fig. 5B for *C. jejuni* and Fig. 5C for *C. coli*. As seen in Fig. 5B, the inclusivity test with the two other *C. jejuni* strains shows a ΔR_{th} response of 83.9 % (strain KC40) and 96.1 % (strain MB3391) of the template-strain response (C157a). The response to other *Campylobacter* species, different from *C. jejuni*, is markedly lower: Injection of *C. coli* results in a ΔR_{th} percentage of 17.8 %, for *C. lari* it is 24.2 %, and in case of *C. upsaliensis* we find a ΔR_{th} percentage of 14.5 % with respect to the specific response. For the *Campylobacteriales* not belonging to the genus *Campylobacter* (*H. pullorum* and three *Arcobacter* variants), the ΔR_{th} response is below the 3σ level of the baseline.

Fig. 5C contains the cross-selectivity and inclusivity results when the SIP was imprinted with *C. coli* C154a as template strain; the highest ΔR_{th} response is observed for *C. coli* C154a itself with 2.88 °C/W. The response to three other *C. coli* strains (MB3272, MB3363, and MB4182) is less but still *ca.* 60 % and therefore strong enough to be easily detectable. The other *Campylobacter* species (*C. lari*, *upsaliensis* and *jejuni*) gave a weak ΔR_{th} response that does not exceed 20 %. The response to *Arcobacter* and *Helicobacter* is insignificant in the sense that it stays well below the 3σ limit.

Together, these results indicate that the *Campylobacter* SIPs are inclusive as they can bind several strains that belong to the same species. Furthermore, they are selective when it comes to distinguishing between different species of the *Campylobacter* genus with a discrimination ratio of at least 4 to 1. Within the accuracy of the readout method, the SIPs are insensitive to *Helicobacter* and *Arcobacter*, which belong to the *Campylobacterales* order and which have both strong structural similarities with *Campylobacter* itself. The absence of response to the microbiome in the poultry intestines was already shown above in Fig. 4B. Technically speaking, the SIP receptors can be qualified as "species-selective", which is in line with recent results on selected *Enterobacteriaceae* [23]. This means also that size- and shape complementarity between imprints and target cells are insufficient to explain the achieved level of selectivity. Phospholipid residues, transferred to the cavities during the imprinting step, were already identified as potential mediators of the recognition effect [26], and this might explain the selectivity and inclusivity observed in the present work: There is growing evidence that different bacterial species own a characteristic phospholipidome in the sense that the lipids composition of their membranes is a fingerprint for the respective species [71]. A first study on the phospholipidome of *C. jejuni* was published very recently by Cao and co-workers [72], while this information is, to best of our knowledge, not yet available for other *Campylobacter* species. A full understanding of the role of phospholipids might therefore assist in developing rationally designed SIP-type receptor with an engineered inclusivity- and selectivity level.

4. Conclusions

In summary, a refined HTM sensor coupled with synthetic, polymer-based receptors was used for the sensitive and selective detection of two thermotolerant *Campylobacter* species. The biomimetic receptors used in this study were SIPs imprinted with *C. coli* or *C. jejuni*, which were deposited on stainless-steel chips using a soft-lithographic imprinting technique. The sensor has several relevant characteristics: First, the detection principle based on a thermal current does not require labelling of the bacteria, which simplifies the detection process. Second, the sensor reaches detection limits in buffer fluids as low as 1.0 × 10^3 CFU/mL for *C. coli* and 6.6 × 10^3 CFU/mL for *C. jejuni*. We anticipate that this can be brought down further by increasing the number of imprints per unit area, a key to this might be avoiding the transition of template *Campylobacter* to its coccoid shape.

The detection limits obtained with cecal solution are 1.1 × 10^3 CFU/mL for *C. coli* and 2.7 × 10^4 CFU/mL for *C. jejuni*. Preparing these samples does not involve more than dissolving cecal droppings in PBS buffer and a filtering step, both can be done easily at a poultry farm or a slaughterhouse to detect the colonization on-site and as early as possible. Due to the abundant *Campylobacter* concentrations in cecal droppings in case of colonization (10^6 – 10^8 CFU/g), our current detection limits are already low enough to detect such situation from just 1 g of easily collectable cecal droppings. The assay time of less than 60 min, including stabilization and rinsing, is considerably shorter than cell-cultivation tests based on the ISO standard 10272-1:2017. Furthermore, we point out that tests based on lateral flow assays and antibodies can only be used once, while the SIP technology with thermal readout can, in principle, measure continuously for monitoring purposes, for instance in a food-production facility.

Regarding selectivity and inclusivity, it is important to mention that SIP receptors, which are imprinted with a specific strain of a given *Campylobacter* species, also bind other strains of the same species with

almost the same sensor response. This is useful information from a practical perspective because fecal samples from different farms usually contain different strains. At the same time, the sensor responds selectively as the signal for *Campylobacter* species that are different from the imprinted one is 4–10 times lower than the species-selective signal. Furthermore, false-positive results due to *Helicobacter* and *Arcobacter* species are hardly expected as the respective signals stay well below the confidence level while the response to the native microbiome present in the chicken intestines is immeasurably small. Taking all elements together, the as-developed sensor system is now at a stage that is ready for practical evaluation in field studies.

CRediT authorship contribution statement

Stella Givanoudi: Investigation, Formal analysis, Validation, Writing - original draft. **Peter Cornelis:** Methodology, Software, Formal analysis, Data curation. **Geertrui Rasschaert:** Validation, Resources. **Gideon Wackers:** Investigation, Writing - original draft, Visualization. **Heiko Iken:** Resources, Methodology. **David Rolka:** Investigation, Visualization. **Derick Yongabi:** Methodology, Investigation. **Johan Robbens:** Funding acquisition, Supervision. **Michael J. Schöning:** Supervision, Resources, Writing - review & editing. **Marc Heyndrickx:** Conceptualization, Methodology, Resources, Supervision, Writing - review & editing, Project administration, Funding acquisition. **Patrick Wagner:** Conceptualization, Methodology, Resources, Supervision, Project administration, Funding acquisition, Visualization, Writing - review & editing.

Declaration of Competing Interest

The authors report no declarations of interest.

Acknowledgements

This research was financially supported by ILVO and the AgrEUfood project, which is funded by the Interreg VA Flanders – The Netherlands program, under CCI grant no. 2014TC16RFCB046, and received co-funding from Provincie Antwerpen and VLAIO (Flanders Innovation & Entrepreneurship). We acknowledge the CAMPREVENTproject (RT 17/2) funded by the Federal Public Service of Health, Food Chain Safety and Environmentfor the chicken cecal samples and a variety of *Campylobacter* strains. KU Leuven is acknowledged for funding *via* the project “Smart Cellular scaffolds” (C14/15/66).

Appendix A. Supplementary data

Supplementary material related to this article can be found, in the online version, at doi:https://doi.org/10.1016/j.snb.2021.129484.

References

[1] M.D. Kirk, S.M. Pires, R.E. Black, M. Caipo, J.A. Crump, B. Devleesschauwer, D. Döpfer, A. Fazil, C.L. Fischer-Walker, T. Hald, A.J. Hall, K.H. Keddy, R.J. Lake, C.F. Lanata, P.R. Torgerson, A.H. Havelaar, F.J. Angulo, World Health Organization estimates of the global and regional disease burden of 22 foodborne bacterial, protozoal, and viral diseases, 2010: a Data Synthesis, PLoS Med. 12 (2015) e1001921, https://doi.org/10.1371/journal.pmed.1001921.

[2] EFSA and ECDC (European Food Safety Authority and European Centre for Disease Prevention and Control), The European Union summary report on trends and sources of zoonoses, zoonotic agents and food-borne outbreaks in 2017, Efsa J. 16 (12) (2018) 5500, https://doi.org/10.2903/j.efsa.2018.5500, 1–262.

[3] J. Robyn, G. Rasschaert, F. Pasmans, M. Heyndrickx, Thermotolerant *Campylobacter* during broiler rearing: risk factors and intervention, Compr. Rev. Food Sci. Food Saf. 14 (2015) 81–105, https://doi.org/10.1111/1541-4337.12124.

[4] E.M. Nielsen, Occurrence and strain diversity of thermophilic *Campylobacters* in cattle of different age groups in dairy herds, Lett. Appl. Microbiol. 35 (2002) 85–89, https://doi.org/10.1046/j.1472-765x.2002.01143.x.

[5] T. Alter, F. Gaull, S. Kasimir, M. Gürtler, H. Mielke, M. Linnebur, K. Fehlhaber, Prevalences and transmission routes of *Campylobacter* spp. strains within multiple pig farms, Vet. Microbiol. 108 (2005) 251–261, https://doi.org/10.1016/j.vetmic.2005.03.004.

[6] C. Zweifel, M.A. Zychowska, R. Stephan, Prevalence and characteristics of Shiga toxin-producing *Escherichia coli*, *Salmonella* spp. and *Campylobacter* spp. isolated from slaughtered sheep in Switzerland, Int. J. Food Microbiol. 92 (2004) 45–53, https://doi.org/10.1016/j.ijfoodmicro.2003.07.005.

[7] J. Baker, M.D. Barton, J. Lanser, *Campylobacter* species in cats and dogs in South Australia, Aust. Vet. J. 77 (1999) 662–666, https://doi.org/10.1111/j.1751-0813.1999.tb13159.x.

[8] G. Rasschaert, L. De Zutter, L. Herman, M. Heyndrickx, *Campylobacter* contamination of broilers: the role of transport and slaughterhouse, Int. J. Food Microbiol. 322 (2020) 108564, https://doi.org/10.1016/j.ijfoodmicro.2020.108564.

[9] I. Sampers, I. Habib, L. De Zutter, A. Dumoulin, M. Uyttendaele, Survival of *Campylobacter* spp. in poultry meat preparations subjected to freezing, refrigeration, minor salt concentration, and heat treatment, Int. J. Food Microbiol. 137 (2010) 147–153, https://doi.org/10.1016/j.ijfoodmicro.2009.11.013.

[10] EFSA Panel on Biological Hazards (BIOHAZ), Scientific opinion on quantification of the risk posed by broiler meat to human campylobacteriosis in the EU, Efsa J. 8 (1) (2010) 1–89, https://doi.org/10.2903/j.efsa.2010.1437, 1437.

[11] OECD/FAO, World Meat Projections, 2019. https://www.oecd-ilibrary.org/sites/22712dab-en/index.html?itemId=/content/component/22712dab-en.

[12] OECD/FAO, Agricultural Outlook 2018-2027, 2018. http://www.fao.org/publications/oecd-fao-agricultural-outlook/2018-2027/en/.

[13] E. Mateo, J. Cárcamo, M. Urquijo, I. Perales, A. Fernández-Astorga, Evaluation of a PCR assay for the detection and identification of *Campylobacter jejuni* and *Campylobacter coli* in retail poultry products, Res. Microbiol. 156 (2005) 568–574, https://doi.org/10.1016/j.resmic.2005.01.009.

[14] N. Botteldoorn, E.V. Coillie, V. Piessens, G. Rasschaert, L. Debruyne, M. Heyndrickx, L. Herman, W. Messens, Quantification of *Campylobacter* spp. in chicken carcass rinse by real-time PCR, J. Appl. Microbiol. 105 (2008) 1909–1918, https://doi.org/10.1111/j.1365-2672.2008.03943.x.

[15] International Organization for Standardization, Microbiology of the Food Chain – Horizontal Method for Detection and Enumeration of *Campylobacter* spp. – Part 1: Detection Method, 2017. https://www.iso.org/standard/63225.html.

[16] P. Vizzini, M. Braidot, J. Vidic, M. Manzano, Electrochemical and optical biosensors for the detection of *Campylobacter* and *Listeria*: an update look, Micromachines 10 (2019), https://doi.org/10.3390/mi10080500.

[17] T. Seliwiorstow, A. Duarte, J. Baré, N. Botteldoorn, K. Dierick, M. Uyttendaele, L. De Zutter, Comparison of sample types and analytical methods for the detection of highly *Campylobacter*-colonized broiler flocks at different stages in the poultry meat production chain, Foodborne Pathog. Dis. 12 (2015) 399–405, https://doi.org/10.1089/fpd.2014.1894.

[18] M.G. Mason, P.J. Blackall, J.R. Botella, J.M. Templeton, An easy-to-perform, culture-free *Campylobacter* point-of-management assay for processing plant applications, J. Appl. Microbiol. 128 (2020) 620–629, https://doi.org/10.1111/jam.14509.

[19] Romer Labs, Description of RapidChek® Campylobacter Test Kit. https://www.romerlabs.com/en/analytes/food-pathogens/campylobacter-testing/.

[20] Microgen Bioproducts Ltd, Description of Campylobacter Latex Agglutination Kit. https://microgenbioproducts.com/microgen-latex-agglutination-kits/.

[21] Microgen Bioproducts Ltd, Description of Singlepath® Campylobacter Latex Agglutination Kit, 2020. https://www.merckmillipore.com/BE/fr/product/Singlepath-Campylobacter,MDA_CHEM-104143?ReferrerURL=https%3A%2F%2Fwww.google.com%2F.

[22] S. Chen, X. Chen, L. Zhang, J. Gao, Q. Ma, Electrochemiluminescence detection of *Escherichia coli* O157: H7 based on a novel polydopamine surface imprinted polymer biosensor, ACS Appl. Mater. Interfaces 9 (2017) 5430–5436, https://doi.org/10.1021/acsami.6b12455.

[23] P. Cornelis, S. Givanoudi, D. Yongabi, H. Iken, S. Duwé, O. Deschaume, J. Robbens, P. Dedecker, C. Bartic, M. Wübbenhorst, M.J. Schöning, M. Heyndrickx, P. Wagner, Sensitive and specific detection of *E. coli* using biomimetic receptors in combination with a modified heat-transfer method, Biosens. Bioelectron. 136 (2019) 97–105, https://doi.org/10.1016/j.bios.2019.04.026.

[24] B. van Grinsven, K. Eersels, O. Akkermans, S. Ellermann, A. Kordek, M. Peeters, O. Deschaume, C. Bartic, H. Diliën, E. Steen Redeker, P. Wagner, T.J. Cleij, Label-free detection of *Escherichia coli* based on thermal transport through surface imprinted polymers, ACS Sens. 1 (2016) 1140–1147, https://doi.org/10.1021/acssensors.6b00435.

[25] E. Yilmaz, D. Majidi, E. Ozgur, A. Denizli, Whole cell imprinting based *Escherichia coli* sensors: a study for SPR and QCM, Sens. Actuators B Chem. 209 (2015) 714–721, https://doi.org/10.1016/j.snb.2014.12.032.

[26] D. Yongabi, M. Khorshid, P. Losada-Pérez, K. Eersels, O. Deschaume, J. D'Haen, C. Bartic, J. Hooyberghs, R. Thoelen, M. Wübbenhorst, P. Wagner, Cell detection by surface imprinted polymers SIPs: a study to unravel the recognition mechanisms, Sens. Actuators B Chem. 255 (2018) 907–917, https://doi.org/10.1016/j.snb.2017.08.122.

[27] K. Eersels, B. van Grinsven, A. Ethirajan, S. Timmermans, K.L. Jiménez Monroy, J. F.J. Bogie, S. Punniyakoti, T. Vandenryt, J.J.A. Hendriks, T.J. Cleij, M.J. Daemen, V. Somers, W. De Ceuninck, P. Wagner, Selective identification of macrophages and cancer cells based on thermal transport through surface-imprinted polymer layers, ACS Appl. Mater. Interfaces 5 (2013) 7258–7267, https://doi.org/10.1021/am401605d.

[28] O. Hayden, K.J. Mann, S. Krassnig, F.L. Dickert, Biomimetic ABO blood-group typing, Angew. Chem. Int. Ed. 45 (2006) 2626–2629, https://doi.org/10.1002/anie.200502857.

[29] F.L. Dickert, O. Hayden, R. Bindeus, K.J. Mann, D. Blaas, E. Waigmann, Bioimprinted QCM sensors for virus detection-screening of plant sap, Anal. Bioanal. Chem. 378 (2004) 1929–1934, https://doi.org/10.1007/s00216-004-2521-5.
[30] C. Tancharoen, W. Sukjee, C. Thepparit, T. Jaimipuk, P. Auewarakul, A. Thitithanyanont, C. Sangma, Electrochemical biosensor based on surface imprinting for Zika virus detection in serum, ACS Sens. 4 (2019) 69–75, https://doi.org/10.1021/acssensors.8b00885.
[31] G. Lautner, J. Kaev, J. Reut, A. Öpik, J. Rappich, V. Syritski, R.E. Gyurcsányi, Selective artificial receptors based on micropatterned surface-imprinted polymers for label-free detection of proteins by SPR imaging, Adv. Funct. Mater. 21 (2011) 591–597, https://doi.org/10.1002/adfm.201001753.
[32] K. Eersels, P. Lieberzeit, P. Wagner, A review on synthetic receptors for bioparticle detection created by surface-imprinting techniques - from principles to applications, ACS Sens. 1 (2016) 1171–1187, https://doi.org/10.1021/acssensors.6b00572.
[33] S. Piletsky, F. Canfarotta, A. Poma, A.M. Bossi, S. Piletsky, Molecularly imprinted polymers for cell recognition, Trends Biotechnol. 38 (2020) 368–387, https://doi.org/10.1016/j.tibtech.2019.10.002.
[34] I. Perçin, N. Idil, M. Bakhshpour, E. Yılmaz, B. Mattiasson, A. Denizli, Microcontact imprinted plasmonic nanosensors: powerful tools in the detection of *Salmonella paratyphi*, Sensors 17 (2017) 1375, https://doi.org/10.3390/s17061375.
[35] F.L. Dickert, O. Hayden, K.P. Halikias, Synthetic receptors as sensor coatings for molecules and living cells, Analyst 126 (2001) 766–771, https://doi.org/10.1039/B009893K.
[36] M. Golabi, F. Kuralay, E.W.H. Jager, V. Beni, A.P.F. Turner, Electrochemical bacterial detection using poly(3-aminophenylboronic acid)-based imprinted polymer, Biosens. Bioelectron. 93 (2017) 87–93, https://doi.org/10.1016/j.bios.2016.09.088.
[37] E. Steen Redeker, K. Eersels, O. Akkermans, J. Royakkers, S. Dyson, K. Nurekeyeva, B. Ferrando, P. Cornelis, M. Peeters, P. Wagner, H. Diliën, B. van Grinsven, T. J. Cleij, Biomimetic bacterial identification platform based on thermal wave transport analysis (TWTA) through surface-imprinted polymers, ACS Infect. Dis. 3 (2017) 388–397, https://doi.org/10.1021/acsinfecdis.7b00037.
[38] R. Schirhagl, E.W. Hall, I. Fuereder, R.N. Zare, Separation of bacteria with imprinted polymeric films, Analyst. 137 (2012) 1495–1499, https://doi.org/10.1039/C2AN15927A.
[39] K. Ren, N. Banaei, R.N. Zare, Sorting inactivated cells using cell-imprinted polymer thin films, ACS Nano 7 (2013) 6031–6036, https://doi.org/10.1021/nn401768s.
[40] D. Wei, O.A. Oyarzabal, T.S. Huang, S. Balasubramanian, S. Sista, A.L. Simonian, Development of a surface plasmon resonance biosensor for the identification of *Campylobacter jejuni*, J. Microbiol. Methods 69 (2007) 78–85, https://doi.org/10.1016/j.mimet.2006.12.002.
[41] N.A. Masdor, Z. Altintas, I.E. Tothill, Surface plasmon resonance immunosensor for the detection of *Campylobacter jejuni*, Chemosensors 5 (2017) 16, https://doi.org/10.3390/chemosensors5020016.
[42] A.D. Taylor, J. Ladd, Q. Yu, S. Chen, J. Homola, S. Jiang, Quantitative and simultaneous detection of four foodborne bacterial pathogens with a multi-channel SPR sensor, Biosens. Bioelectron. 22 (2006) 752–758, https://doi.org/10.1016/j.bios.2006.03.012.
[43] Z. Dehghani, J. Mohammadnejad, M. Hosseini, B. bakhshi, A.H. Rezayan, Whole cell FRET immunosensor based on graphene oxide and graphene dot for *Campylobacter jejuni* detection, Food Chem. 309 (2020) 125690, https://doi.org/10.1016/j.foodchem.2019.125690.
[44] K.E. Sapsford, A. Rasooly, C.R. Taitt, F.S. Ligler, Detection of *Campylobacter* and *Shigella* species in food samples using an array biosensor, Anal. Chem. 76 (2004) 433–440, https://doi.org/10.1021/ac035122z.
[45] S. Viswanathan, C. Rani, J.A. Ho, Electrochemical immunosensor for multiplexed detection of food-borne pathogens using nanocrystal bioconjugates and MWCNT screen-printed electrode, Talanta 94 (2012) 315–319, https://doi.org/10.1016/j.talanta.2012.03.049.
[46] J. Huang, G. Yang, W. Meng, L. Wu, A. Zhu, X. Jiao, An electrochemical impedimetric immunosensor for label-free detection of *Campylobacter jejuni* in diarrhea patients' stool based on O-carboxymethylchitosan surface modified Fe_3O_4 nanoparticles, Biosens. Bioelectron. 25 (2010) 1204–1211, https://doi.org/10.1016/j.bios.2009.10.036.
[47] Y.J. Kim, H.-S. Kim, J.W. Chon, D.H. Kim, J.Y. Hyeon, K.H. Seo, New colorimetric aptasensor for rapid on-site detection of *Campylobacter jejuni* and *Campylobacter coli* in chicken carcass samples, Anal. Chim. Acta 1029 (2018) 78–85, https://doi.org/10.1016/j.aca.2018.04.059.
[48] M. Khorshid, P. Losada-Pérez, P. Cornelis, M. Dollt, S. Ingebrandt, C. Glorieux, F. U. Renner, B. van Grinsven, W. De Ceuninck, R. Thoelen, P. Wagner, Searching for a common origin of heat-transfer effects in bio- and chemosensors: a study on thiols as a model system, Sens. Actuators B Chem. 310 (2020) 127627, https://doi.org/10.1016/j.snb.2019.127627.
[49] K. Eersels, B. van Grinsven, M. Peeters, T.J. Cleij, P. Wagner, Heat transfer as a new sensing technique for the label-free detection of biomolecules, in: M.J. Schöning, A. Poghossian (Eds.), Label-Free Biosensing, Springer, Cham (Switzerland), 2017, pp. 383–407, https://doi.org/10.1007/978-3-319-75220-4.
[50] B. van Grinsven, K. Eersels, M. Peeters, P. Losada-Pérez, T. Vandenryt, T.J. Cleij, P. Wagner, The heat-transfer method: a versatile low-cost, label-free, fast, and user-friendly readout plat-form for biosensor applications, ACS Appl. Mater. Interfaces 6 (2014) 13309–13318, https://doi.org/10.1021/am503667s.
[51] T. Nakano, G. Kikugawa, T. Ohara, A molecular dynamics study on heat conduction charac-teristics in DPPC lipid bilayer, J. Chem. Phys. 133 (2010), https://doi.org/10.1063/1.3481650.
[52] B. van Grinsven, N. Vanden Bon, H. Strauven, L. Grieten, M. Murib, K.L. Jiménez Monroy, S.D. Janssens, K. Haenen, M.J. Schöning, V. Vermeeren, M. Ameloot, L. Michiels, R. Thoelen, W. De Ceuninck, P. Wagner, Heat-transfer resistance at solid-liquid interfaces: a tool for the detection of single-nucleotide polymorphisms in DNA, ACS Nano 6 (2012) 2712–2721, https://doi.org/10.1021/nn300147e.
[53] K. Betlem, S. Hoksbergen, N. Mansouri, M. Down, P. Losada-Pérez, K. Eersels, B. van Grinsven, T.J. Cleij, P. Kelly, D. Sawtell, M. Zubko, C. Banks, M. Peeters, Real-time analysis of microbial growth by means of the heat-transfer method (HTM) using *Saccharomyces cerevisiae* as model organism, Phys. Med. 6 (2018) 1–8, https://doi.org/10.1016/j.phmed.2018.05.001.
[54] K. Eersels, B. van Grinsven, M. Khorshid, V. Somers, C. Püttmann, C. Stein, S. Barth, H. Diliën, G.M. Bos, W.T. Germeraad, Heat-transfer-method-based cell culture quality assay through cell detection by surface imprinted polymers, Langmuir 31 (2015) 2043–2050, https://doi.org/10.1021/la5046173.
[55] P. Losada-Pérez, K.L. Jiménez-Monroy, B. Van Grinsven, J. Leys, S.D. Janssens, M. Peeters, C. Glorieux, J. Thoen, K. Haenen, W. De Ceuninck, P. Wagner, Phase transitions in lipid vesicles detected by a complementary set of methods: heat-transfer measurements, adiabatic scanning calorimetry, and dissipation-mode quartz crystal microbalance, Phys. Status Solidi Appl. Mater. Sci. 211 (2014) 1377–1388, https://doi.org/10.1002/pssa.201431060.
[56] D. Hermans, F. Pasmans, W. Messens, A. Martel, F. Van Immerseel, G. Rasschaert, M. Heyndrickx, K. Van Deun, F. Haesebrouck, Poultry as a host for the zoonotic pathogen *Campylobacter jejuni*, Vector Borne Zoonotic Dis. 12 (2012) 89–98, https://doi.org/10.1089/vbz.2011.0676.
[57] S.K. Yadav, Dose-response models to understand toxicodynamics for pollutants in ecosystems, Environ. Sci. 4 (2013) 77–80.
[58] Camprevent project, Belgian Federal Public Service of Health, Food Chain Safety and Environment DGZ [Accessed 28 July 2020], 2020, https://www.dgz.be/project/camprevent.
[59] J. Silva, D. Leite, M. Fernandes, C. Mena, P.A. Gibbs, P. Teixeira, *Campylobacter* spp. as a foodborne pathogen: a review, Front. Microbiol. 2 (2011) 200, https://doi.org/10.3389/fmicb.2011.00200.
[60] P. Tangwatcharin, S. Chanthachum, P. Khopaibool, M.W. Griffiths, Morphological and physiological responses of *Campylobacter jejuni* to stress, J. Food Prot. 69 (2006) 2747–2753, https://doi.org/10.4315/0362-028X-69.11.2747.
[61] E. Frirdich, J. Biboy, M. Pryjma, J. Lee, S. Huynh, C.T. Parker, S.E. Girardin, W. Vollmer, E.C. Gaynor, The *Campylobacter jejuni* helical to coccoid transition involves changes to peptide-glycan and the ability to elicit an immune response, Mol. Microbiol. 112 (2019) 280–301, https://doi.org/10.1111/mmi.14269.
[62] E. Oh, L. McMullen, B. Jeon, Impact of oxidative stress defense on bacterial survival and morphological change in *Campylobacter jejuni* under aerobic conditions, Front. Microbiol. 6 (2015) 295, https://doi.org/10.3389/fmicb.2015.00295.
[63] N. Ikeda, A.V. Karlyshev, Putative mechanisms and biological role of coccoid form formation in *Campylobacter jejuni*, Eur. J. Microbiol. Immunol. (Bp) 2 (2012) 41–49, https://doi.org/10.1556/EuJMI.2.2012.1.7.
[64] P. Keblinski, J.A. Eastman, D.G. Cahill, Nanofluids for thermal transport, Mater. Today 8 (2005) 36–44, https://doi.org/10.1016/S1369-7021(05)70936-6.
[65] J.A. Eastman, S.U.S. Choi, S. Li, W. Yu, L.J. Thompson, Anomalously increased effective thermal conductivities of ethylene glycol-based nanofluids containing copper nanoparticles, Appl. Phys. Lett. 78 (2001) 718–720, https://doi.org/10.1063/1.1341218.
[66] J.T. Beery, M.B. Hugdahl, M.P. Doyle, Colonization of gastrointestinal tracts of chicks by *Campylobacter jejuni*, Appl. Environ. Microbiol. 54 (1988) 2365–2370, https://doi.org/10.1128/AEM.54.10.2365-2370.1988.
[67] S. Wei, M. Morrison, Z. Yu, Bacterial census of poultry intestinal microbiome, Poult. Sci. 92 (2013) 671–683, https://doi.org/10.3382/ps.2012-02822.
[68] R.G. Zanoni, M. Rossi, D. Giacomucci, V. Sanguinetti, G. Manfreda, Occurrence and antibiotic susceptibility of *Helicobacter pullorum* from broiler chickens and commercial laying hens in Italy, Int. J. Food Microbiol. 116 (2007) 168–173, https://doi.org/10.1016/j.ijfoodmicro.2006.12.007.
[69] A. Sirianni, N.O. Kaakoush, M.J. Raftery, H.M. Mitchell, The pathogenic potential of *Helicobacter pullorum*: possible role for the type VI secretion system, Helicobacter 18 (2013) 102–111, https://doi.org/10.1111/hel.12009.
[70] N. Ertas, Y. Dogruer, Z. Gonulalan, A. Guner, I. Ulger, Prevalence of *Arcobacter* species in drinking water, spring water, and raw milk as determined by multiplex PCR, J. Food Prot. 73 (2010) 2099–2102, https://doi.org/10.4315/0362-028x-73.11.2099.
[71] C. Sohlenkamp, O. Geiger, Bacterial membrane lipids: diversity in structures and pathways, FEMS Microbiol. Rev. 40 (2016) 133–159, https://doi.org/10.1093/femsre/fuv008.
[72] X. Cao, J.F.H.M. Brouwers, L. van Dijk, C.H.A. van de Lest, C.T. Parker, S. Huynh, J.P.M. van Putten, D.J. Kelly, M.M.S.M. Wösten, The unique phospholipidome of the enteric pathogen *Campylobacter jejuni*: lysophosholipids are required for motility at low oxygen availability, J. Mol. Biol. 432 (2020) 5244–5258, https://doi.org/10.1016/j.jmb.2020.07.012.

Stella Givanoudi received the M.Sc. degree in Pharmaceutical Biotechnology - Molecular Diagnostics from Aristotle University of Thessaloniki (Greece) in 2015, and she is currently a Ph.D. candidate in the Arenberg Doctoral School at KU Leuven, Belgium. Her research projects were a collaboration between the Flanders Research Institute for Agriculture, Fisheries, and Food (ILVO) and the Laboratory for Soft Matter and Biophysics of KU Leuven. Her research interests include the development of biosensors for the detection and quantification of small molecules and micro-organisms.

Peter Cornelis obtained a Master degree in Biomedical Sciences at Hasselt University (Belgium) in 2014 and defended his Ph.D. in Sciences at KU Leuven in 2019 with a thesis on bacterial detection by thermal methods in combination with biomimetic receptors. Thereafter, he was a postdoctoral researcher focusing on impedimetric biodetection for food- and environmental-safety applications.

Geertrui Rasschaert obtained her Ph.D. in 2007 at Ghent University (Belgium) titled 'The molecular epidemiology of *Salmonella* and *Campylobacter* during poultry transport and slaughter'. Since 2007, she is working as senior researcher at Flanders Research Institute for Agriculture, Fisheries and Food (ILVO), where her main interests are bacteriological zoonoses, use of antimicrobials and antimicrobial resistance in the primary production, molecular techniques and gastro-intestinal fermentation systems to mimic the gastro-intestinal gut of animals.

Gideon Wackers obtained a master in Bioelectronics and Nanotechnology from the University of Hasselt (Belgium) in 2014. He is currently a research associate at KU Leuven, Belgium, where he works within the Laboratory for Soft Matter and Biophysics at the Department of Physics and Astronomy. His research focusses on molecular and surface imprinted polymer based biosensors for both medical and food safety applications.

Heiko Iken studied biomedical engineering at the Aachen University of Applied Sciences (Germany) from 2003 to 2007. After finishing his diploma degree (Dipl.-Ing.) at the Institute of Nano- and Biotechnologies, he started as a process engineer, focusing mainly on sensor fabrication in cleanroom environment.

David Rolka received his diploma degree (Dipl.-Ing.) in Biomedical Engineering in 2003 from the University of Applied Sciences Aachen (Germany). His main research interests are field-effect-based chemical sensors, flow-injection analysis systems, and imaging techniques for biofunctional surfaces and interfaces.

Derick Yongabi obtained a Master of Biomedical Science in Bioelectronics and Nanotechnology from the University of Hasselt (Belgium) in 2015 and completed Postgraduate Studies in Advanced Medical Imaging at KU Leuven (Belgium) in 2018. He also holds a Master of Science in Research Methods from the University of Leeds (United Kingdom, 2011). He is currently a research associate at KU Leuven, where he works within the Laboratory for Soft Matter and Biophysics at the Department of Physics and Astronomy. His research exploits interdisciplinary scientific knowledge and tools for understanding cellular interactions towards biosensors and biomedical applications.

Johan Robbens obtained his Ph.D. in Molecular Biology in 1994 at the Ghent University (Belgium) on "Solubility of heterologous proteins overexpressed in *E. coli*". He conducted post-docs in the fields of proteomics and environmental toxicology at the same university. At Antwerp University (Belgium), he was Industrial Research Fellow, dealing with the valorization of science in environmental toxicology. Since 2009, he is a tenured researcher at the Flanders Research Institute for Agriculture, Fisheries and Food (ILVO, Belgium), where he is the head of the cells 'Blue Biotech' and 'FoodIntegrity'. His research interests are valorization of marine resources for agricultural and industrial applications as well as rapid methods to detect food safety compounds or organisms. He also holds a MBA diploma from KU Leuven. He is visiting research leader at University Antwerp.

Michael J. Schöning received his PhD in 1993 at Karlsruhe University of Technology (Germany) in the field of semiconductor-based microsensors for the detection of ions in liquids. From 1993 until 1999, he has been with the Institute of Thin Films and Interfaces (now, Institute of Biological Information Processing (IBI-3)) at the Research Center Jülich, and since 1999, he was appointed as full Professor at Aachen University of Applied Sciences, Campus Jülich. Since 2006, he serves as a director of the Institute of Nano- and Biotechnologies (INB) at the Aachen University of Applied Sciences. His main research subjects concern silicon-based chemical and biological sensors, thin-film technologies, solid-state physics, microsystem and nano(bio-)technology.

Marc Heyndrickx has done his Ph.D. in Microbiology in 1991 at the Ghent University (Belgium) on *Clostridium* anaerobic fermentations and conducted a post-doc in the same lab on the revision and improvement of the *Bacillus* taxonomy by a polyphasic approach. Since 1997, he is a tenured researcher at the Institute of Agricultural and Fisheries Research (ILVO, Belgium), where he leads as scientific director from 2002 onwards a research team on food safety. His research interests are chemical and microbiological food safety, with a special emphasis on detection, identification, typing, virulence, antibiotic resistance and remediation of zoonotic foodborne pathogens as well as spoilage organisms in food. He is visiting professor of bacterial zoonoses at the Faculty of Veterinary Medicine of the Ghent University.

Patrick Wagner obtained a Ph.D. in physics at the Technical University Darmstadt (Germany) in 1994; thereafter, he received a Marie Curie postdoctoral fellowship and became a professor of biophysics at Hasselt University in 2001. Since 2014, he is a full professor at KU Leuven with a research focus on the development of label-free bioanalytical sensors for medical diagnostics and food safety. His special attention goes to synthetic bioreceptors such as molecularly- and surface-imprinted polymers in combination with electronic- and thermal detection principles. Until date, more than 20 researchers completed their Ph.D. successfully within his team; he is (co-) author of 300 publications and (co-) inventor of 7 granted patents, mainly in the field of biodetection based on heat-transfer effects.